

Responses to reviewer comments

We thank the reviewers for their detailed, helpful, and overall supportive comments. We have revised the manuscript to account for each comment. Responses to the individual comments are provided below. Reviewer comments are in **bold**. Author responses are in plain text. Modifications to the manuscript are in *italics*. Line numbers in the response correspond to those in the revised manuscript text file.

Reviewer #1

This manuscript presents chemical analysis results of submicron organic aerosols in Beijing during summer. It mainly uses two types of aerosol mass spectrometers and compares the measurement results with each other. Due to different detection schemes, the authors found that the OA determined by SP-AMS are quite different from that of HR-AMS OA. In particular, vehicle-related OA might be detected more by SP-AMS; cooking OA, was not associated with BC; a unique biomass burning OA, on the other hand, was only significantly observed on BC cores. The work provides valuable contribution into understanding the chemical behaviors and therefore the impacts on air quality and climate of OA. It can be accepted for publication in ACP, this reviewer has however a few minor comments as listed below:

(1) There are a few typos, grammar or format errors in the manuscript that should be corrected, for example, in Line 38, Line 67, Line 79, Line 235-236, Line299, etc.

Thanks for the comment. The typos, grammar, and format errors in the manuscript mentioned above were corrected, and a thorough check is also conducted to correct other errors

(2) Line 114: it is not clear what is the “BC-free species” referring to.

Now we changed it to non-BC containing particles.

(3) Line 114-116: Explain a bit more why HR-AMS can measure Type I and II, and SP-AMS for Type II and III.

We added a sentence in Lines 117-121: "*NR-PM₁ can be quickly vaporized by the 600 °C tungsten vaporizer of HR-AMS and be detected. The SP-AMS used here was equipped only with the Nd-YAG intra-cavity infrared laser (1064 nm) (tungsten vaporizer was physically removed), it can selectively detect BC-containing particles only, which include Type II and Type III species.*

(4) Line 150-155: Did you perform corrections, for example, on elemental ratios, between the two AMS as you state there could be some mass spectral differences due to measurement schemes?

Yes, scaling factors of 1.10 for H:C and 0.86 for O:C by Canagaratna et al. 2015 were applied.

(5) Line 248: I suggest to delete this sentence.

As suggested, this sentence is removed.

(6) Line 280-282: As you state that HOA quantification might be influenced by the changes of collection efficiency. Can you explain a bit more about the possible influences of the collection efficiency on other OA factors?

The possible influences on CE has been described in Lines 151-155: "It should be noted that the BC quantification will not be affected by particle bouncing without the tungsten vaporizer, which could affect the CE in the standard HR-AMS measurements (Canagaratna et al., 2007). However, the CE will be governed by the overlap of the particle beam and laser beam (Lee et al., 2017; Massoli et al., 2015; Willis et al., 2014)."

(7) Line 320: Is it possible that the A-BBOA fraction (for example, <5%) in total NR-PM₁ is too low to be resolved by the PMF?

Yes, this is possible. The A-BBOA might be included in the NR-PM₁ MO-OOA as described in Lines 321-323.

(8) Figure 6: It is better to put the legends adjacent to the HR-AMS and SP-AMS plots directly in d, to make it clear.

Done

Reviewer #2

Wang et al. compare the OA properties by parallel measurements using SP-AMS and HR-AMS respectively, in summer Beijing. The AMS technique is suitable for online quantification of OA and in particular SP-AMS can provide a unique piece of OA that coated on rBC cores. The findings are therefore unique and valuable to understand the OA composition and chemistry in megacities like Beijing. The overall interpretation of the data is reasonable and the paper is well written, I suggest its acceptance in ACP after the following minor issues are well addressed.

(1) During the APHH campaign, another type of mass spectrometer (single particle mass spectrometry) was used to elucidate the OA properties too. Some studies should be included here to facilitate the interpretation.

Thanks for the suggestion, we have added two references by using single particle MS techniques in the revised manuscript.

Chen, Y.; Cai, J.; Wang, Z.; Peng, C.; Yao, X.; Tian, M.; Han, Y.; Shi, G.; Shi, Z.; Liu, Y.; Yang, X.; Zheng, M.; Zhu, T.; He, K.; Zhang, Q.; Yang, F. Simultaneous measurements of urban and rural particles in Beijing – Part 1: Chemical composition and mixing state. *Atmos. Chem. Phys.*, 20, 9231-9247, 10.5194/acp-20-9231-2020, 2020a.

Chen, Y.; Shi, G.; Cai, J.; Shi, Z.; Wang, Z.; Yao, X.; Tian, M.; Peng, C.; Han, Y.; Zhu, T.; Liu, Y.; Yang, X.; Zheng, M.; Yang, F.; Zhang, Q.; He, K. Simultaneous measurements of urban and rural particles in Beijing – Part 2: Case studies of haze events and regional transport. *Atmos. Chem. Phys.*, 20, 9249-9263, 10.5194/acp-20-9249-2020, 2020b.

(2) Some typos or citation formats do not follow the ACP style, please check and revise.

We have carefully checked the manuscript.

(3) In the instrumentation section, some necessary technical details are missing. For example, what is the m/z range of the OA mass spectra for HR-AMS and SP-AMS? Time resolution? Operation modes (V or W?) Is the tungsten vaporizer physically removed or turned off in SP-AMS?

Thanks for the comment. The m/z range of the OA mass spectra for HR-AMS and SP-AMS reported in this study is across m/z 12-120 as described in Lines 161. The operation mode is described in Lines 153-154 as well. However, we added a statement for technical details in Lines 123-125: “*Briefly, the two AMS were operated under the mass quantify favorable mode (V-mode) with a time resolution of five minutes.*” And a statement in 117-121: ”*NR-PM1 can be flash vaporization via the 600 °C tungsten*

vaporizer of HR-AMS and thus to be detected. For BC-containing particles, due to the SP-AMS equipped a Nd-YAG intra-cavity infrared laser (1064 nm) module, it can selectively detect BC-containing particles (Type II and Type III) with the tungsten vaporizer be moved.”

(4) Xie et al (Atmos Environ 2019; 213:499-504) shows different PMF results from this study, is it because the datasets used for PMF analysis are different?

There are two reasons for the difference of PMF results between this study and the one reported by Xie et al. One reason is caused by the different PMF inputs. For example, in Xie's report, only carbon clusters and OA mass spectra were used in the PMF analysis, while ion fragments from inorganic species (e.g., SO₄²⁻, NO₃⁻, NO₂⁺, Cl⁺, HCl⁺, NH₄⁺, and NH₂⁺) were also included in the PMF analysis. Another reason is because of the amount of dataset, in Xie's study, there are only 9 days (from June 4 to 13), while there are 26 day (from June 4 to 30).

(5) Line 316-319: The ABBOA is not separated in the HR-AMS dataset, is it likely because that the ABBOA contains more refractory components?

Although this can be investigated further but we think it is unlikely. Most organics are non-refractory and there is no specific reason that BBOA contains more refractory components than other types of OA. In addition, according to previous studies of SP-AMS, the evaporation of non-BC species associated with BC core are under lower temperature. The reason why the A-BBOA was not separated in HR-AMS measure OA might be caused by its low mass fraction in the total OA (but not that low in BC-PM₁ OA), for example, less than 5% of total OA.

(6) References: Line 504-516, the references are the same, but repeated twice.

Corrected.

(7) Figure 5: There are only four ion families here. How about the nitrogen-containing organic ions, although they may have little influences?

The nitrogen-containing organic ion fragments were also involved in the PMF analysis as shown in the Figure 2, however, those signals are relatively very low, and for better comparison, nitrogen-containing organic ion fragments were not shown here.

Characterization of **Submicron Organic Particles** **submicron organic particles** in Beijing **During Summertime** **during summertime**: Comparison **Between** **between** SP-AMS and HR-AMS

带格式的: 左侧: 3.17 厘米, 右侧: 3.17 厘米, 指定行网格

Junfeng Wang^{1,2,*}, Jianhuai Ye², Dantong Liu³, Yangzhou Wu³, Jian Zhao⁴, Weiqi Xu⁴, Conghui Xie⁴, Fuzhen Shen¹, Jie Zhang⁵, Paul E. Ohno², Yiming Qin², Xiuyong Zhao⁶, Scot T. Martin², Alex K.Y. Lee⁷, Pingqing Fu⁸, Daniel J. Jacob², Qi Zhang⁹, Yele Sun⁴, Mindong Chen¹ and Xinlei Ge^{1,*}

¹Jiangsu Key Laboratory of Atmospheric Environment Monitoring and Pollution Control, Collaborative Innovation Center of Atmospheric Environment and Equipment Technology, School of Environmental Science and Engineering, Nanjing University of Information Science and Technology, Nanjing, China

²School of Engineering and Applied Sciences, Harvard University, Cambridge, MA, United States

³Department of Atmospheric Sciences, School of Earth Sciences, Zhejiang University, Hangzhou, China

⁴State Key Laboratory of Atmospheric Boundary Layer Physics and Atmospheric Chemistry, Institute of Atmospheric Physics, Chinese Academy of Sciences, Beijing, China

⁵Department of Atmospheric Science, Colorado State University, Fort Collins, CO, United States

⁶State Environmental Protection Key Laboratory of Atmospheric Physical Modeling and Pollution Control, State Power Environmental Protection Research Institute, Nanjing, China

⁷Department of Civil and Environmental Engineering, National University of Singapore, Singapore

⁸Institute of Surface-Earth System Science, Tianjin University, Tianjin, China

⁹Department of Environmental Toxicology, University of California Davis, Davis, CA, United States

*Corresponding author: Xinlei Ge (Email: caxinra@163.com); Junfeng Wang (Email: wangjunfeng@g.harvard.edu).

1 ABSTRACT

2 Black carbon (BC) particles in Beijing summer haze play an important role in
3 regional radiation balance and related environmental processes. Understanding the
4 factors that lead to variability ~~in~~^{of} the impacts of BC remains limited. Here, we present
5 observations by a soot-particle aerosol mass spectrometer of BC-containing submicron
6 particulate matter (BC-PM₁) in ~~the summer of 2017 in~~ Beijing, China during 2017
7 summer. These observations were compared to concurrently measured total non-
8 refractory submicron particulate matter (NR-PM₁) by a high-resolution aerosol mass
9 spectrometer (HR-AMS). Distinct properties were observed between NR-PM₁ and BC-
10 PM₁ ~~related relevant~~ to organic aerosol (OA) composition ~~with hydrocarbon~~.
11 Hydrocarbon-like OA in BC-PM₁ was found to be up to two-fold higher than that in
12 NR-PM₁ in fresh vehicle emissions, suggesting that a part of HOA in BC-PM₁ may be
13 overestimated, likely due to the change of ~~the~~ collection efficiency of SP-AMS.
14 Cooking-related OA was only identified in NR-PM₁, whereas aged biomass burning
15 OA (A-BBOA) was a unique factor only identified in BC-PM₁. The A-BBOA was
16 linked to those heavily coated BC, which may lead to enhancement of light absorption
17 ability of BC by a factor of two via the “lensing effect”. More-oxidized oxygenated OA
18 identified in BC-containing particles was found to be slightly different from that
19 observed by HR-AMS, mainly due to the influence of A-BBOA. Overall, these findings
20 highlight that BC in urban Beijing is ~~partly~~^{partially} of agricultural fire origin and, a
21 unique biomass burning-related OA associated with BC may be ubiquitous in aged BC-
22 PM₁, and this OA may play a role in affecting air quality and climate that has not
23 previously been fully considered.

24 **1. Introduction**

25 Black carbon (BC) is an important component of atmospheric aerosol that exerts
26 negative effects on regional radiation balance (Bond et al., 2013) and human health
27 (Janssen, 2012). It absorbs solar radiation, leading to direct atmospheric heating
28 (Ramanathan and Carmichael, 2008). Indirectly, BC-containing particles (BCc) can
29 also serve as cloud condensation nuclei upon mixing with hydrophilic species (e.g.,
30 sulfate), resulting in changes in cloud properties (Wu et al., 2019). Inhalation of BC is
31 associated with adverse health impacts such as respiratory diseases and birth defects
32 (Janssen, 2012). (Bond et al., 2013) and human health (Janssen, 2012). It absorbs solar
33 radiation, leading to direct atmospheric heating (Ramanathan and Carmichael, 2008).
34 Indirectly, BC-containing particles (BCc) can also serve as cloud condensation nuclei
35 upon mixing with hydrophilic species (e.g., sulfate), resulting in changes in cloud
36 properties (Wu et al., 2019). Inhalation of BC is associated with adverse health impacts
37 such as respiratory diseases and birth defects (Janssen, 2012).

38 BC particles are released to the atmosphere directly and usually mixed with non-
39 BC materials (e.g., inorganic and organic) from incomplete fuel combustion and open
40 fires (Ramanathan and Carmichael, 2008; Bond et al., 2013; Chen et al.,
41 2013). (Ramanathan and Carmichael, 2008; Bond et al., 2013; Chen et al., 2013). Non-
42 BC species also can coat onto primary BCc in the atmosphere through condensation
43 and/or coagulation processes (Lee et al., 2017). (Lee et al., 2017). These atmospheric
44 processes gradually alter the mixing state and the morphology (e.g., from an externally-
45 mixed fractal structure (Buseck et al., 2014) into an internally mixed “core shell”
46 structure (China et al., 2015)) of BCc. (Buseck et al., 2014) into an internally-mixed
47 “core-shell” structure (China et al., 2015)) of BCc. These alterations can enhance the
48 light absorption capacity of the BC core via the “lensing effect” due to the increased
49 light absorption cross-section as a result of the enhanced coating thickness (Saleh et al.,
50 2015; Cappa et al., 2012). (Saleh et al., 2015; Cappa et al., 2012). Additionally, the
51 chemical constituents of BCc may dynamically change during the aging processes,
52 which also lead to changes in the light absorption capacity of the particles (Wang et al.,
53 2019; Wang et al., 2017). (Wang et al., 2019; Wang et al., 2017). Because these physical

54 and chemical processes of both organic and inorganic species inside BCc continuously
55 alter particle properties throughout the lifetime of the particles, great uncertainty
56 remains in quantifying the light absorption ability of BC (Liu et al., 2018; Liu et al.,
57 2019). (Liu et al., 2018; Liu et al., 2019). Understanding the relationship of mixing state
58 and chemical composition to the light absorption properties of BCc, as well as its
59 spatiotemporal distribution, is of importance to accurately evaluate the impacts of BC
60 in regional air quality.

61 Aerodyne high-resolution aerosol mass spectrometry (HR-AMS) (Canagaratna et
62 al., 2007) (Canagaratna et al., 2007) has been widely applied in field studies to
63 investigate the chemically-resolved composition of non-refractory submicron
64 particulate matter (NR-PM₁, species that vaporize at temperature < 600 °C) (Li et al.,
65 2015; Lee et al., 2013; Sun et al., 2012; Ge et al., 2012b; Ge et al., 2012a; Xu et al.,
66 2019c; Sun et al., 2014). (Li et al., 2015; Lee et al., 2013; Sun et al., 2012; Ge et al.,
67 2012b; Ge et al., 2012a; Xu et al., 2019b; Sun et al., 2014). However, the working
68 temperature of the standard HR-AMS tungsten vaporizer (600 °C) is not sufficient to
69 vaporize refractory species such as BC. To overcome this limitation, soot-particle
70 aerosol mass spectrometry (SP-AMS) is developed (Onasch et al., 2012). (Onasch et al.,
71 2012). In addition to the standard tungsten vaporizer, SP-AMS is equipped with a laser
72 vaporizer (with a wavelength of 1064 nm) which selectively heats BC (core), together
73 with the non-BC species mixed with it (Wang et al., 2016). (Wang et al., 2016). This
74 novel technique makes it possible to compare the compositions of submicron BCc (BC-
75 PM₁) and NR-PM₁, allowing a more accurate assessment of the impacts of BC.
76 However, a question is whether the ion fragments of organic species ionized by the
77 70eV electron impact of SP-AMS and HR-AMS are the same in terms of different
78 thermal schemes. It has been reported that the mass spectra of NR-PM₁ organic have
79 high m/z 44 (mainly CO₂⁺) signal, while the mass spectra of BC-related organics have
80 high m/z 43 (C₃H₇⁺ and C₂H₅O⁺) signal. The reason for this is the SP-AMS provides
81 vaporization of the BC-PM₁ at lower temperatures compared to the standard tungsten
82 vaporizer of the HR-AMS, resulting in less overall fragmentation and therefore less
83 CO₂⁺ production in the laser, in addition, the lower fragmentation also causes the

84 presence of more ion fragments at $m/z > 100$ amu in the SP-AMS mass spectra
85 compared to that of HR-AMS (Canagaratna et al., 2015b; Massoli et al.,
86 2015). (Canagaratna et al., 2015b; Massoli et al., 2015). Nevertheless, quantification of
87 BC-PM₁ organic aerosol (OA) factors identified from positive matrix factorization
88 (PMF) has been reported that were not significantly affected by the differences of mass
89 spectra between HR-AMS and SP-AMS (Lee et al., 2017; Massoli et al., 2015). (Lee et
90 al., 2017; Massoli et al., 2015).

91 To date, there have only been a few studies that have compared the differences of
92 species in BC-PM₁ and NR-PM₁ (Lee et al., 2017; Collier et al., 2015; Massoli et al.,
93 2015). Lee et al. (Lee et al., 2017; Collier et al., 2015; Massoli et al., 2015). Lee et al.
94 found that cooking-related organic aerosol (COA) may externally mix with BC in
95 summertime California (Lee et al., 2017). (Lee et al., 2017). The COA factor was
96 identified in NR-PM₁ organic aerosol (OA), but not in the BC-related OA. Wang et al
97 found that transported biomass burning organic aerosol could be thickly coated on BC
98 in central Tibetan Plateau and significantly enhance the light absorption capacity of BC
99 cores (Wang et al., 2017). (Wang et al., 2017). Interestingly, the transported biomass
100 burning organic aerosol was not resolved in NR-PM₁ OA particles from concurrent HR-
101 AMS measurements (Xu et al., 2018). (Xu et al., 2018). These studies suggest that BC-
102 related OA may undergo different atmospheric processes compared to those do not
103 contain BC.

104 Beijing is a megacity known for high particulate matter (PM) concentrations. BC-
105 PM₁ during haze events of summertime Beijing may have distinct sources and
106 properties than other locations in the world. As a part of the UK-China Air Pollution
107 and Human Health (APHH) project summer campaign (Shi et al., 2019). (Shi et al., 2019;
108 Chen et al., 2020a; Chen et al., 2020b). in this study, we focus on the differences of
109 individual species between BC-PM₁ and NR-PM₁ regarding their chemical composition,
110 mass loadings, sources, and formation pathways in summertime in urban Beijing.
111 Results from this study provide a better understanding of the formation mechanism of
112 OA particles in Beijing haze and valuable insights in assessing their impacts on air
113 quality.

114

115 2. Experiments

116 2.1. Sampling site and period

117 The observations were conducted at a rooftop laboratory (8 m above ground level)
118 in the Tower Division of the Institute of Atmospheric Physics (IAP), Chinese Academy
119 of Sciences (CAS) in urban Beijing (39°58'N, 116°22'E), China, from 4 to 29 June,
120 2017. This site has been reported multiple times to be a typical urban observation
121 location (Xie et al., 2019b; Liu et al., 2019; Wang et al., 2019; Qiu et al., 2019; Xu et al.,
122 2019a; Xie et al., 2019a). (Xie et al., 2019b; Liu et al., 2019; Wang et al., 2019; Qiu et al.,
123 2019; Xu et al., 2019a; Xie et al., 2019a). The site is located around the North 3rd Ring
124 Road of Beijing. A highway is approximately 360 m to the east and a lot of restaurants
125 (e.g., Sichuan style and BBQ) are within 100 m on the north side.

126

127 2.2. Instrumentation

128 Two Aerodyne Aerosol Mass Spectrometers (AMS), including a laser-only Soot-
129 Particle AMS (SP-AMS) and a High-Resolution Time of Flight AMS (HR-AMS) were
130 deployed to measure chemical compositions and size distributions of BC-PM₁ and NR-
131 PM₁, respectively. Three types of species were measured during the campaign: NR-
132 PM₁, including BC-free non-refractory species that don't mix with BC (Type I) and non-
133 refractory species that mixed with BC (Type II), and BC-PM₁ (BC core and both
134 refractory and non-refractory species coated on the core) (Type III). NR-PM₁ can be
135 quickly vaporized by the 600 °C tungsten vaporizer of HR-AMS is capable of
136 measuring Type I and Type II, while laser only and be detected. The SP-AMS can
137 measure used here was equipped only with the Nd-YAG intra-cavity infrared laser
138 (1064 nm) (tungsten vaporizer was physically removed), it can selectively detect BC-
139 containing particles only, which include Type II and Type III species. A shared PM_{2.5}
140 cyclone inlet (Model URG-2000-30ED) with 3 Lpm flowrate and a diffusion dryer were
141 used prior to the sampling. The detailed information on the operation of HR-AMS and
142 SP-AMS during the sampling campaign can be found in previous literature (Xie et al.,
143 2019a; Xu et al., 2019a). (Xie et al., 2019a; Xu et al., 2019b). Details of tuning,

带格式的: 突出显示

带格式的: 突出显示

带格式的: 突出显示

带格式的: 突出显示

带格式的: 突出显示

带格式的: 突出显示

144 calibration, and configurations of the two AMS instruments can be seen in our previous
145 papers (Wang et al., 2019; Xu et al., 2019a; Xu et al., 2019d). (Wang et al., 2019; Xu et
146 al., 2019a; Xu et al., 2019b). The two AMS were operated under the V-mode which is
147 favorable for mass quantification with a time resolution of five minutes. Mixing ratios
148 of O₃, and NO₂ (Thermo Fisher Scientific, model 49i and model 42C) were measured
149 in parallel simultaneously. Vertical meteorological parameters, including temperature
150 (T) and relative humidity (RH), were measured from the IAP 325m meteorological
151 tower.

152

153 **2.3. Data Analysis**

154 AMS data analysis was performed by using Squirrel 1.57 and Pika 1.16I based on
155 Igor Pro 6.37 (WaveMetrics Corp.). The measurement of filtered air was performed for
156 24 hours before the start of the campaign to determine the detection limits of various
157 aerosol species and to adjust the fragmentation table. The relative ionization efficiency
158 (RIE) of BC was calibrated with Regal Black (RB, REGAL 400R pigment black, Cabot
159 Corp.). The average ratio of C₁⁺ to C₃⁺ ionized from pure BC (RB) was determined to
160 be 0.53, which minimizes the influence of C₁⁺ from non-refractory organics. The RIE
161 of BC was determined to be 0.17 based on calibrations performed before, in the middle,
162 and at the end of the campaign. RIEs of NO₃⁻, SO₄²⁻, NH₄⁺ were determined to be 1.1,
163 0.82, and 3.82, respectively, and default values of 1.3 and 1.4 for RIEs of Chl and Org
164 were applied, respectively (Canagaratna et al., 2007). (Canagaratna et al., 2007).
165 Consistent with BC-PM₁ measurements in previous studies, the RIEs calibration of
166 NO₃⁻, SO₄²⁻, NH₄⁺ were performed before the tungsten vaporizer was removed, by
167 assuming those RIEs remain unchanged throughout the campaign (Wang et al.,
168 2017). (Wang et al., 2017). Polystyrene latex (PSL) spheres (100-700 nm) (Duke
169 Scientific Corp., Palo Alto, CA) were used to calibrate the particle size distribution
170 before the campaign. The collection efficiency (CE) of 0.5 were applied for both HR-
171 AMS and SP-AMS in this study. It should be noted that, the BC quantification will not
172 be affected by particle bouncing without the tungsten vaporizer, which could affect the
173 CE in the standard HR-AMS measurements (Canagaratna et al., 2007). (Canagaratna et

174 al., 2007). However, the CE will be governed by the overlap of particle beam and laser
175 beam (Lee et al., 2017;Massoli et al., 2015;Willis et al., 2014).(Lee et al., 2017;Massoli
176 et al., 2015;Willis et al., 2014). Both HR-AMS and SP-AMS resolved mass
177 concentrations of NR-PM₁ and BC were calculated based on V-mode high-resolution
178 fitting. Due to different vaporization schemes between the HR-AMS and SP-AMS,
179 mass spectra from these two instruments even for the same population of aerosols are
180 not entirely the same. Because laser-only SP-AMS generally results in less overall
181 fragmentation, its mass profile may contain more large *m/z* fragments and less small
182 *m/z* fragments compared to that from HR-AMS(Massoli et al., 2015).(Massoli et al.,
183 2015). In addition, the elemental ratios of organics reported here, i.e., oxygen-to-carbon
184 and hydrogen-to-carbon ratios (O/C and H/C) were calculated based ~~the “Improved-~~
185 ~~Ambient (I-A)” method~~(Canagaratna et al., 2015a).on the “Improved-Ambient (I-A)”
186 method(Canagaratna et al., 2015a) (scaling factors of 1.10 for H:C and 0.86 for O:C
187 were applied for elemental ratios calculated from SP-AMS data)

188 ~~Positive matrix factorization (PMF)~~(Paatero and Tapper, 1994)~~Positive matrix~~
189 factorization (PMF)(Paatero and Tapper, 1994) was performed on the high-resolution
190 organic mass spectra matrix of both NR-PM₁ and BC-PM₁ (e.g., BC (C_x⁺), and species
191 associated with BC) across *m/z* 12–120 using PMF Evaluation Tool written in Igor
192 (Ulbrich et al., 2009), ~~following the standard procedure~~(Zhang et al., 2011). ~~Four types~~
193 ~~of organic aerosol (OA) from total NR-PM₁ (see our previous paper)~~(Xu et al., 2019e)
194 ~~and five OA factors from BC-PM₁ were identified~~(Ulbrich et al., 2009), ~~following the~~
195 ~~standard procedure~~(Zhang et al., 2011). ~~Four types of organic aerosol (OA) from total~~
196 ~~NR-PM₁ (see our previous paper)~~(Xu et al., 2019b) and ~~five OA factors from BC-PM₁~~
197 ~~were identified~~. C_x⁺ was involved in the calculation of elemental ratios (e.g., O/C and
198 H/C) of PMF OA factors. All data presented in this paper were averaged hourly and are
199 presented at local time (Beijing Time, UTC+8).

200

201 3. Results and discussion

202 3.1. Overview of observations

203 Figure 1 shows the temporal variations of selected chemical species during the

204 campaign. Information for other variables is provided in the supplementary materials
205 (SM). The two cases labeled in Figure 1 are of interest. Case I (June 8-13) was
206 characterized with high NO₂ concentrations (average 26.7 ± 13.5 ppb, Table S1) and
207 relatively low O₃ concentrations (41.7 ± 30.0 ppb) with NO₂-to-O₃ ratio of 0.64. Case
208 II (June 17-22) was featured by low NO₂ (14.9 ± 5.9 ppb) and high O₃ (84.6 ± 30.6 ppb)
209 concentrations with an NO₂-to-O₃ ratio of 0.18. Unlike winter Beijing haze pollution,
210 RH remained at a relatively low level ($36.5 \pm 15.3\%$), which is not expected to play a
211 significant role in OA formation during the campaign (Figure 1b and Figure S1). In
212 contrast, a strong correlation has been observed between temperature and O₃ ($r^2 = 0.53$).
213 The temperature was higher on average in Case II (29.8 ± 3.8 °C) than in Case I (26.1
214 ± 4.1 °C).

215 The mass concentrations and mass concentration ratios of organic (Org), sulfate
216 (SO₄²⁻) and nitrate (NO₃⁻) in NR-PM₁ (in solid line) and BC-PM₁ (in dotted line) are
217 shown in Figures 1c-e. High correlations were observed between BC-PM₁ and NR-PM₁
218 measurements for SO₄²⁻ ($r^2 = 0.70$) and NO₃⁻ ($r^2 = 0.86$), but not for Org ($r^2 = 0.49$).
219 This result suggests that, BC-PM₁ Org has distinct sources or formation pathways from
220 NR-PM₁ Org. Comparing two cases, the average mass ratios of BC-PM₁ to NR-PM₁ for
221 SO₄²⁻ and NO₃⁻ in Case I (0.24 ± 0.11 and 0.37 ± 0.12) were close to those in Case II
222 (0.19 ± 0.06 and 0.31 ± 0.07). However, ratios of BC-PM₁ to NR-PM₁ for Org were a
223 factor of greater for Case I (0.74 ± 0.32) compare to Case II (0.46 ± 0.13). During the
224 nighttime, this ratio increases to almost unity in Case I. Additionally, BC concentration
225 in Case I (average 2.6 ± 1.6 $\mu\text{g m}^{-3}$) was 1.5 folds higher than in Case II (average $1.7 \pm$
226 $0.8\mu\text{g m}^{-3}$). The implication is that the organic is mostly associated with BC and likely
227 comprised of freshly emitted compounds in Case I. This is also evident by the moderate
228 correlation between NO₂ and BC-PM₁ Org ($r^2 = 0.42$) in Case I. On the other hand, the
229 lower Org ratio in Case II with higher O₃ concentrations indicates greater oxidation and
230 secondary processes in non-BC particles.

231

232 **3.2. Source apportionment of BC-PM₁ OA**

233 To further investigate the differences between organics in NR-PM₁ and BC-PM₁,

234 the comparison of PMF OA factors between NR-PM₁ and BC-PM₁ Org is necessary.
235 Four factors were identified from PMF analysis of the NR-PM₁ Org matrix, including
236 hydrocarbon-related OA (HOA), cooking OA (COA), less-oxidized oxygenated OA
237 (LO-OOA), and more-oxidized oxygenated OA (MO-OOA). [Details of the NR-PM₁ PMF analysis can be found in our previous study \(Xu et al., 2019d\)](#).[Details of the NR-PM₁ PMF analysis can be found in our previous study \(Xu et al., 2019b\)](#). Here we only
238 present the PMF results of the SP-AMS measured BC-PM₁ Org. As shown in Figure 2,
239 five factors were resolved by PMF with factors including a HOA, a less oxidized OOA
240 (OOA1), three more-oxidized OOA factors were recombined into one OOA factor
241 (MO-OOA= Aged- biomass burning organic aerosol (A-BBOA) + OOA2 + OOA3).
242 Diagnostic plots of this PMF solution is presented in Figure S2.

243 HOA consists of a series of hydrocarbon fragments ($C_xH_y^+$) in its mass spectrum
244 (Figure 2f), thus having a low O/C ratio (0.13) but [a](#) high H/C ratio (1.62). It has a r^2 of
245 0.92 with $C_4H_9^+$ (m/z = 57) and a r^2 of 0.57 with NO_x (Figure 2a), indicative of its
246 sources from vehicle emissions[\(Xu et al., 2019b\)](#).[\(Xu et al., 2019a\)](#). It also correlated
247 tightly with BC (r^2 of 0.70) and a series of polycyclic aromatic hydrocarbons (PAHs)
248 ions, e.g., $C_9H_7^+$ (m/z 115, r^2 of 0.63).

249 The second factor has a remarkably high fraction of the biomass burning organic
250 aerosol (BBOA) marker ions of $C_2H_4O_2^+$ (m/z = 60) (1.31%) and $C_3H_5O_2^+$ (m/z = 73)
251 (1.34%) in its mass spectrum (Figure 2g), much higher than that observed in non-BBOA
252 (e.g., 0.3% at m/z = 60) in previous studies [\(Sun et al., 2016; Xu et al., 2019b; Wang et al., 2017\)](#).[\(Sun et al., 2016; Xu et al., 2019a; Wang et al., 2017\)](#). As expected, the
253 temporal variation of this factor correlated tightly with those of $C_2H_4O_2^+$ and $C_3H_5O_2^+$
254 (r^2 of 0.71 and 0.72, respectively). In addition, the mass spectrum of this factor is
255 strikingly similar to that of the transported BBOA which was observed at a remote site
256 in the central Tibetan Plateau [\(Wang et al., 2017\)](#),[\(Wang et al., 2017\)](#), with a r^2 of 0.97.
257 Here we categorized the transported BBOA as aged-BBOA (A-BBOA) identified in
258 this study. Similar to the A-BBOA observed in Tibetan Plateau, which has an O/C ratio
259 of 0.51, this factor also has a relatively high O/C ratio of 0.48, greater than that of
260 primary BBOA (O/C of 0.18–0.26)[\(Wang et al., 2017\)](#).[\(Wang et al., 2017\)](#). These
261

264 findings support that the second factor may be associated with the oxidation of biomass
265 burning emissions. The temporal variation of ABBOA in the Tibetan Plateau was
266 reported to be highly correlated with the potassium ion fraction (K^+ , r^2 of 0.78), and
267 $K_3SO_4^+$ (r^2 of 0.92). However, the temporal variation of the second factor in this study
268 is only correlated well with that of $K_3SO_4^+$ (r^2 of 0.64) but not K^+ (r^2 of 0.01). The
269 reason for this phenomenon is that the major source of K^+ in remote sites like the
270 Tibetan Plateau was long-distance transport of K_2SO_4 particles, which probably from
271 biomass burning-related K-containing salts interacts with H_2SO_4 (V. Buxton et al.,
272 1999)-(Buxton et al., 1999). In contrast, there are multiple primary sources of K^+ in
273 PM₁ (e.g., diesel-vehicle emissions, and mainly KCl particles) in urban areas (Figure
274 S3). Based on these observations, $K_3SO_4^+$ could be defined as an external A-BBOA
275 indicator. Moreover, a previous transmission electron microscopy study also
276 showed that significant agricultural BBOA was mixed with soot and transport
277 from the North China Plain to urban Beijing, meanwhile, K_2SO_4 was also identified
278 within those impact single BBOA soot particles (Li et al., 2010)-single BBOA-soot
279 particles (Li et al., 2010). Hence, this second factor is identified as A-BBOA that was
280 subjected to oxidation during transport to the measurement area as presented in the fire-
281 point map and three-day back trajectories (Figure S4). June should be the month of
282 maximum agricultural related biomass burning in the North China Plain, although we
283 thought that this burning had been banned in recent years because of air quality
284 concerns (Shen et al., 2019). The implication is that the effectiveness of banning straw
285 burning may be overestimated with maximum agricultural-related biomass burning in
286 the North China Plain, although we thought that such burning activities had been
287 banned in recent years (Shen et al., 2019).

288 The OOA1 factor has an O/C of 0.28 (Figure 2h). Similar to the NR-PM₁-LO-
289 OOA(Xu et al., 2019c),The OOA1 factor has an O/C of 0.28 (Figure 2h). Similar to the
290 NR-PM₁ LO-OOA (Xu et al., 2019b), it is highly correlated with $C_2H_3O^+$ (r^2 of 0.72).
291 The $C_2H_3O^+$ ion (m/z = 43) is an important component of secondary organic aerosol
292 (SOA)(Collier et al., 2015;Ng et al., 2011)(Collier et al., 2015;Ng et al., 2011) and the
293 diurnal patterns of the OOA1 and $C_2H_3O^+$ both show a great enhancement around

带格式的: 突出显示

294 noontime (Figure S5), indicating the importance of secondary formation of less
295 oxidized organic aerosol through daytime photochemical activity.

296 The OOA2 factor has an O/C of 0.42 (Figure 2i) and the OOA3 factor has a smaller
297 O/C of 0.32 (Figure 2j). OOA2 correlated strongly with sulfate (r^2 of 0.92; Figure 2d)
298 and OOA3 correlated highly with nitrate (r^2 of 0.97; Figure 2e). These features agree
299 well with the ~~previously~~previous observation for low-volatility OOA (sulfate-related
300 OOA) and semi-volatile OOA (nitrate-related OOA) in Tibetan Plateau ~~(Wang et al.,~~
301 2017).~~(Wang et al., 2017).~~

302 **3.3. Comparison of NR-PM₁ and BC-PM₁ OA factors**

303 The sum of the above-mentioned BC-PM₁ A-BBOA, OOA2, and OOA3 fractions
304 is comparable to the NR-PM₁ MO-OOA factor, based on their high O/C ratios. Figures
305 3a-c are comparisons of the mass loadings of HOA, LO-OOA, and MO-OOA in both
306 NR-PM₁ and BC-PM₁. NR-PM₁ HOA, LO-OOA, and MO-OOA are strongly correlated
307 with their counterpart fractions of BC-PM₁, with r^2 values of 0.68, 0.60, and 0.61,
308 respectively. In Case I, most of the time, the mass loadings of BC-PM₁ HOA and MO-
309 OOA are higher than those in NR-PM₁, while LO-OOA shows the opposite trend. In
310 Case II, the mass loadings of BC-PM₁ HOA are also generally higher than those of NR-
311 PM₁ HOA, however, NR-PM₁ MO-OOA and LO-OOA are almost two folds higher than
312 those of BC-PM₁. Figures 3d-f are comparisons of the fractions of HOA, LO-OOA, and
313 MO-OOA in NR-PM₁ and non-BC material in BC-PM₁ (coatings), respectively. In Case
314 I, the fractions of HOA and MO-OOA internally-mixed with BC are almost two times
315 and four times higher, respectively, than those in NR-PM₁, whereas the two LO-OOA
316 fractions closely track each other. In Case II, two LO-OOA fractions are still overlapped,
317 but compared to Case I, the fraction of HOA in BC-PM₁ coatings is over four times that
318 of NR-PM₁ HOA, and the difference between the two MO-OOA fractions is smaller.

319 As shown in Figure 4, the average of BC-PM₁ HOA fractions (0.27 ± 0.17 and 0.11 ± 0.07 , respectively) are higher than those in NR-PM₁ (0.12 ± 0.08 and 0.02 ± 0.02 , respectively) in both Case I and Case II, indicating that HOA particles is more internally
320 mixed with BC compared to other OA materials. However, the possibility that RIE of
321 OA coating may be lower than the default RIE value should also be considered.

322 The average mass loadings of NR-PM₁ LO-OOA in both Case I and Case II were
323 higher than those of BC-PM₁. However, the fraction of LO-OOA in both NR-PM₁ and
324 BC-PM₁ coatings were very close to each other during the two cases, with an average
325 value of 0.23 ± 0.10 and 0.25 ± 0.12 , respectively, indicating that the probability of LO-
326 OOA condensation onto the two different types of particles is similar.

327 A greater difference between the MO-OOA fractions in NR-PM₁ and BC-PM₁ was
328 observed in Case I than in Case II, and there is more MO-OOA in BC-PM₁ than in NR-
329 PM₁ in Case I. A similar comparison between NR-PM₁ MO-OOA with BC-PM₁ MO-

332 OOA without A-BBOA can be found in SI (Figure S6), which shows closer fractions in
333 both Case I and Case II. Therefore, one possibility which that may cause higher MO-
334 OOA fraction in BC-PM₁ than that in NR-PM₁ in Case I is the presence of the BC-PM₁
335 A-BBOA, which is only identified from the BC-PM₁ OA. More details of the BC-PM₁
336 A-BBOA are discussed in Section 3.4.

337

338 **3.4. Characteristics of A-BBOA in BC-containing PM₁**

339 Figure 5 shows the high-resolution mass spectra of A-BBOA observed in Nam Co
340 (June 2015) and Beijing (June 2017) by laser-only SP-AMS. A mass spectra very
341 similar to that observed in Beijing was also observed in Nanjing (February 2017)(Wu
342 et al., 2019),(Wu et al., 2019), with a r^2 of 0.95. The A-BBOA observed in Nam Co
343 (the Tibetan Plateau) was found in the thickest coated and internally-mixed BC-PM₁
344 (the mass ratio of coatings to BC core (R_{BC}) can reach 14), which enhances the light
345 absorption ability (E_{abs}) of the BC core by a factor of 1.5 to 2.0 via the “lensing effect”.

346 As shown in Figure 6, A-BBOA was associated with those large particles ($D_{va} >$
347 300nm) which were also heavily-coated ($R_{BC} > 9$, Figure 6a and 6c). Because A-BBOA
348 is a moderately aged OA, the OSc was very steady when $R_{BC} > 9$ (Figure 6c). Figure
349 6b presents the fractions of the OA factors (left) and the degree of light absorption
350 enhancement (E_{abs} , estimated by the mass ratios of BC measured by Aethalometer
351 model 33 and SP-AMS), as a function of R_{BC} . Figure 6d shows the temporal variations
352 of the fractions of NR-PM₁ OA and BC-PM₁ OA from 15:00 to 24:00 on June 17, 2017
353 when the highest A-BBOA concentrations were observed. There is a significant
354 enhancement of A-BBOA which may account for up to 60% of the total OA coatings,
355 which could enhance the BC-PM₁ MO-OOA fraction (within the purple frame in the
356 bottom panel of Figure 6d).

357 In this study, A-BBOA was only observed by SP-AMS and was indeed only
358 associated with BC. It is likely that A-BBOA was emitted together with BC when
359 burning biomass fuel, and was oxidized subsequently during the transport. However,
360 we cannot exclude the possibility that A-BBOA can be detected by HR-AMS. For
361 example, it might be included in NR-PM₁ MO-OOA factor. Without separating A-

362 BBOA from other organic species, the source apportionment for HR-AMS may obscure
363 air-quality- and climate-related implications of A-BBOA in the atmosphere, such as the
364 enhancement of aerosol light absorption ability (Figure 6b).

365 **4. Conclusions and implications**

366 Online chemical characteristics of BC and its associated species was for the first
367 time elucidated in urban Beijing in summer, and compared with those of NR-PM₁
368 species. The biggest difference between the two measurements was in the composition
369 of the organic species. In particular, we found BC in urban Beijing in June is partially
370 of agricultural fire origin and, an unique biomass burning-related OA factor (A-BBOA)
371 which was moderately aged, only existed in thickly coated BC-PM₁ ($R_{BC} > 9$), but not
372 NR-PM₁. The unique A-BBOA could make up a significant portion of BC coating
373 material. ~~In addition to Beijing, similar A-BBOA was also identified in other locations,
374 such as central Tibet Plateau (Wang et al., 2017) and Nanjing (Wu et al., 2019); In
375 addition to Beijing, similar A-BBOA was also identified in other locations, such as
376 central Tibet Plateau (Wang et al., 2017) and Nanjing (Wu et al., 2019),~~ suggesting that
377 it may be ubiquitously present in BC-PM₁ in ambient atmosphere.

378 BBOA species are known to constitute a large portion of light-absorbing organics
379 (brown carbon, BrC). The delay of BBOA oxidation and its longer duration time on BC
380 cores can extend the impacts of BC. Moreover, together with our previous study of BC-
381 associated A-BBOA in Tibet, results presented herein demonstrate that A-BBOA could
382 lead to thick coating on BC cores, meaning a significant “lensing effect” to the
383 enhancement of BC light absorption ~~(Liu et al., 2017); (Liu et al., 2017)~~. As a key
384 component of BC coating, presence of this factor may also alter the bulk hygroscopicity
385 of BC-PM₁. It could therefore affect its ability as cloud condensation nuclei (CCN) ~~(Wu
386 et al., 2019); (Wu et al., 2019)~~. Overall, the emission, evolution and transport of such
387 A-BBOA, may influence the atmospheric behaviors and influence the role of BC in the
388 air quality and climate (e.g., radiative forcing and precipitation). We propose that future
389 laboratory, field, and modeling studies are needed to verify the presence of A-BBOA,
390 and to evaluate the regional environmental impacts of it.

391

Data availability. The data in this study are available from the authors upon request
(caxinra@163.com).

Supplement. [The supplement related to this article is available online at: xxx.](#)

带格式的: 字体: 非倾斜

ACKNOWLEDGMENTS

Author contributions. JF, DL, YW, JZ, WX, CX, FS and XG conducted the measurements and analyzed the data. JF, JY and PO wrote the first draft, JZ, PO, YQ, XZ, AL, SM, PF, DJ, QZ, YS, MC and XG contributed to the analyses and improvement of the paper. JF and XG contributed to the revision of the paper.

Competing interests. The authors declare that they have no conflict of interest.

Special issue statement. This article is part of the special issue “In-depth study of air pollution sources and processes within Beijing and its surrounding region (APHH-Beijing) (ACP/AMT inter-journal SI)”. It is not associated with a conference.

Acknowledgements

The authors from PRC acknowledge support from the National Natural Science Foundation of China (21777073) and the National Key Research and Development Program of China (No. 2018YFC0213802). The authors from Harvard and NUIST acknowledge additional support through the Harvard-NUIST Joint Laboratory for Air Quality and Climate (JLAQC).

ABBREVIATIONS

BC Black carbon

PM₁ Particulate matter with an aerodynamic diameter smaller than 1 μm

NR-PM₁ non-refractory PM₁

BC-PM₁ BC-containing particles in PM₁

BrC Brown carbon

HR-AMS High-resolution aerosol mass spectrometer (Aerodyne Research Inc.)

SP-AMS Soot-particle aerosol mass spectrometer (Aerodyne Research Inc.)

IE Ionization efficiency

RIE Relative ionization efficiency
HRMS High-resolution mass spectra
PMF Positive matrix factorization
OA Organic aerosol
SOA Secondary organic aerosol O/C Oxygen-to-carbon ratio
H/C Hydrogen-to-carbon ratio
A-BBOA Aged biomass burning organic aerosol
SV-OOA Semi-volatile oxygenated organic aerosol
LV-OOA low-volatility oxygenated organic aerosol
MO-OOA more-oxidized oxygenated organic aerosol
LO-OOA less-oxidized oxygenated organic aerosol
 R_{BC} mass ratio of BC coatings to BC
 D_{va} Vacuum aerodynamic diameter

REFERENCES

- 392 Bond, T. C., Doherty, S. J., Fahey, D. W., Forster, P. M., Berntsen, T., DeAngelo, B. J., Flanner, M. G.,
393 Ghan, S., Kärcher, B., Koch, D., Kinne, S., Kondo, Y., Quinn, P. K., Sarofim, M. C., Schultz, M. G.,
394 Schulz, M., Venkataraman, C., Zhang, H., Zhang, S., Bellouin, N., Guttikunda, S. K., Hopke, P. K.,
395 Jacobson, M. Z., Kaiser, J. W., Klimont, Z., Lohmann, U., Schwarz, J. P., Shindell, D., Storelvmo, T.,
396 Warren, S. G., and Zender, C. S.: Bounding the role of black carbon in the climate system: A
397 scientific assessment, *J Geophys Res: Atmos.*, 118, 5380–5552, 10.1002/jgrd.50171, 2013.
398 Buseck, P. R., Adachi, K., Gelencsér, A., Tompa, É., and Pósfai, M.: *Ns Soot: A Material-Based Term*
399 *for Strongly Light-Absorbing Carbonaceous Particles*, *Aerosol Science and Technology*, 48, 777–
400 788, 10.1080/02786826.2014.919374, 2014.
401 Canagaratna, M. R., Jayne, J. T., Jimenez, J. L., Allan, J. D., Alfarra, M. R., Zhang, Q., Onasch, T. B.,
402 Drewnick, F., Cee, H., Middlebrook, A., Della, A., Williams, L. R., Trimborn, A. M., Northway, M. J.,
403 DeCarlo, P. F., Kolb, C. E., Davidovits, P., and Worsnop, D. R.: Chemical and microphysical
404 characterization of ambient aerosols with the aerodyne aerosol mass spectrometer, *Mass*
405 *Spectrom Rev.*, 26, 185–222, 10.1002/Mas.20115, 2007.
406 Canagaratna, M. R., Jimenez, J. L., Kroll, J. H., Chen, Q., Kessler, S. H., Massoli, P., Hildebrandt Ruiz,
407 L., Fortner, E., Williams, L. R., Wilson, K. R., Surratt, J. D., Donahue, N. M., Jayne, J. T., and Worsnop,
408 D. R.: Elemental ratio measurements of organic compounds using aerosol mass spectrometry:
409 characterization, improved calibration, and implications, *Atmos. Chem. Phys.*, 15, 253–272,
410 10.5194/acp-15-253-2015, 2015a.
411 Canagaratna, M. R., Massoli, P., Browne, E. C., Franklin, J. P., Wilson, K. R., Onasch, T. B., Kirchstetter,
412 T. W., Fortner, E. C., Kolb, C. E., Jayne, J. T., Kroll, J. H., and Worsnop, D. R.: Chemical Compositions
413 of Black Carbon Particle Cores and Coatings via Soot Particle Aerosol Mass Spectrometry with
414 Photoionization and Electron Ionization, *The Journal of Physical Chemistry A*, 119, 4589–4599,
415 10.1021/jp510711u, 2015b.
416 Cappa, C. D., Onasch, T. B., Massoli, P., Worsnop, D. R., Bates, T. S., Cross, E. S., Davidovits, P.,
417 Hakala, J., Hayden, K. L., Jobson, B. T., Kolesar, K. R., Lack, D. A., Lerner, B. M., Li, S. M., Mellon, D.,
418 Nuaaman, I., Olfert, J. S., Petäjä, T., Quinn, P. K., Song, C., Subramanian, R., Williams, E. J., and Zaveri,
419 R. A.: Radiative absorption enhancements due to the mixing state of atmospheric black carbon,
420 *Science*, 337, 1078–1081, 10.1126/science.1223447, 2012.
421 Chen, B., Andersson, A., Lee, M., Kirillova, E. N., Xiao, Q., Kruså, M., Shi, M., Hu, K., Lu, Z., Streets, D.
422 G., Du, K., and Gustafsson, O.: Source Forensics of Black Carbon Aerosols from China,
423 *Environmental Science & Technology*, 47, 9102–9108, 10.1021/es401599r, 2013.
424 China, S., Scarnato, B., Owen, R. C., Zhang, B., Ampadu, M. T., Kumar, S., Dzepina, K., Dziebak, M.
425 P., Fialho, P., Perlinger, J. A., Hueber, J., Helmig, D., Mazzoleni, L. R., and Mazzoleni, C.: Morphology
426 and mixing state of aged soot particles at a remote marine free troposphere site: Implications for
427 optical properties, *Geophysical Research Letters*, 42, 1243–1250, 10.1002/2014gl062404, 2015.
428 Collier, S., Zhou, S., Kuwayama, T., Forestieri, S., Brady, J., Zhang, M., Kleeman, M., Cappa, C.,
429 Bertram, T., and Zhang, Q.: Organic PM Emissions from Vehicles: Composition, O/C Ratio, and
430 Dependence on PM Concentration, *Aerosol Science and Technology*, 49, 86–97,
431 10.1080/02786826.2014.1003364, 2015.
432 Ge, X., Zhang, Q., Sun, Y., Ruchl, C. R., and Setyan, A.: Effect of aqueous-phase processing on
433 aerosol chemistry and size distributions in Fresno, California, during wintertime, *Environmental*
434 *Chemistry*, 9, 221–235, <http://dx.doi.org/10.1071/EN11168>, 2012a.

- 435 Ge, X. L., Setyan, A., Sun, Y., and Zhang, Q.: Primary and secondary organic aerosols in Fresno,
436 California during wintertime: Results from high resolution aerosol mass spectrometry, *J. Geophys.*
437 *Res.*, 117, D19301, 10.1029/2012jd018026, 2012b.
- 438 Janssen, N., G. N., Miriam; Lanki, Timo; Salonen, Raimo; Cassee, Flemming; Hoek, Gerard;
439 Fischer, Paul; Brunekreef, Bert; Krzyzanowski, Michal: Health effects of black carbon, 2012.
- 440 Lee, A. K. Y., Chen, C. L., Liu, J., Price, D. J., Betha, R., Russell, L. M., Zhang, X., and Cappa, C. D.:
441 Formation of secondary organic aerosol coating on black carbon particles near vehicular emissions,
442 *Atmos. Chem. Phys.*, 17, 15055–15067, 10.5194/acp-17-15055-2017, 2017.
- 443 Lee, B. P., Li, Y. J., Yu, J. Z., Louie, P. K. K., and Chan, C. K.: Physical and chemical characterization
444 of ambient aerosol by HR-ToF-AMS at a suburban site in Hong Kong during springtime 2011,
445 *Journal of Geophysical Research: Atmospheres*, n/a–n/a, 10.1002/jgrd.50658, 2013.
- 446 Li, W. J., Shao, L. Y., and Buseck, P. R.: Haze types in Beijing and the influence of agricultural biomass
447 burning, *Atmos. Chem. Phys.*, 10, 8119–8130, 10.5194/acp-10-8119-2010, 2010.
- 448 Li, Y. J., Lee, B. P., Su, L., Fung, J. C. H., and Chan, C. K.: Seasonal characteristics of fine particulate
449 matter (PM) based on high resolution time of flight aerosol mass spectrometric (HR-ToF-AMS)
450 measurements at the HKUST Supersite in Hong Kong, *Atmos. Chem. Phys.*, 15, 37–53,
451 10.5194/acp-15-37-2015, 2015.
- 452 Liu, C., Chung, C. E., Yin, Y., and Schnaiter, M.: The absorption Ångström exponent of black carbon:
453 from numerical aspects, *Atmos. Chem. Phys.*, 18, 6259–6273, 10.5194/acp-18-6259-2018, 2018.
- 454 Liu, D., Whitehead, J., Alfara, M. R., Reyes Villegas, E., Spracklen, Dominick V., Reddington, Carly L.,
455 Kong, S., Williams, Paul I., Ting, Y. C., Haslett, S., Taylor, Jonathan W., Flynn, Michael J., Morgan,
456 William T., McFiggans, G., Coe, H., and Allan, James D.: Black carbon absorption enhancement in
457 the atmosphere determined by particle mixing state, *Nature Geoscience*, 10, 184–188,
458 10.1038/ngeo2901, 2017.
- 459 Liu, D., Joshi, R., Wang, J., Yu, C., Allan, J. D., Coe, H., Flynn, M. J., Xie, C., Lee, J., and Squires, F.:
460 Contrasting physical properties of black carbon in urban Beijing between winter and summer,
461 *Atmospheric Chemistry and Physics*, 6749–6769, 2019.
- 462 Massoli, P., Onasch, T. B., Cappa, C. D., Nuamaan, I., Hakala, J., Hayden, K., Li, S. M., Sueper, D. T.,
463 Bates, T. S., Quinn, P. K., Jayne, J. T., and Worsnop, D. R.: Characterization of black carbon-
464 containing particles from soot particle aerosol mass spectrometer measurements on the RAV
465 Atlantis during CalNex 2010, *Journal of Geophysical Research: Atmospheres*, 120, 2014JD022834,
466 2015.
- 467 Ng, N. L., Canagaratna, M. R., Jimenez, J. L., Chhabra, P. S., Seinfeld, J. H., and Worsnop, D. R.:
468 Changes in organic aerosol composition with aging inferred from aerosol mass spectra, *Atmos.*
469 *Chem. Phys.*, 11, 6465–6474, 10.5194/acp-11-6465-2011, 2011.
- 470 Onasch, T. B., Trimborn, A., Fortner, E. C., Jayne, J. T., Kok, G. L., Williams, L. R., Davidovits, P., and
471 Worsnop, D. R.: Soot Particle Aerosol Mass Spectrometer: Development, Validation, and Initial
472 Application, *Aerosol Science and Technology*, 46, 804–817, 10.1080/02786826.2012.663948, 2012.
- 473 Paatero, P., and Tapper, U.: Positive matrix factorization: A non-negative factor model with optimal
474 utilization of error estimates of data values, *Environmetrics*, 5, 111–126, 10.1002/env.3170050203,
475 1994.
- 476 Qiu, Y., Xie, Q., Wang, J., Xu, W., Li, L., Wang, Q., Zhao, J., Chen, Y., Chen, Y., Wu, Y., Du, W., Zhou,
477 W., Lee, J., Zhao, C., Ge, X., Fu, P., Wang, Z., Worsnop, D. R., and Sun, Y.: Vertical Characterization
478 and Source Apportionment of Water-Soluble Organic Aerosol with High-resolution Aerosol Mass

- 479 Spectrometry in Beijing, China, *ACS Earth and Space Chemistry*, 3, 273–284,
480 10.1021/acsearthspacechem.8b00155, 2019.
- 481 Ramanathan, V., and Carmichael, G.: Global and regional climate changes due to black carbon,
482 *Nature Geosci.*, 1, 221–227, 2008.
- 483 Saleh, R., Marks, M., Heo, J., Adams, P. J., Donahue, N. M., and Robinson, A. L.: Contribution of
484 brown carbon and lensing to the direct radiative effect of carbonaceous aerosols from biomass
485 and biofuel burning emissions, *Journal of Geophysical Research: Atmospheres*, 120, 10,285–
486 210,296, 10.1002/2015JD023697, 2015.
- 487 Shen, L., Jacob, D. J., Zhu, L., Zhang, Q., Zheng, B., Sulprizio, M. P., Li, K., De Smedt, I., González
488 Abad, G., Cao, H., Fu, T. M., and Liao, H.: The 2005–2016 Trends of Formaldehyde Columns Over
489 China Observed by Satellites: Increasing Anthropogenic Emissions of Volatile Organic Compounds
490 and Decreasing Agricultural Fire Emissions, *Geophysical Research Letters*, 46, 4468–4475,
491 10.1029/2019gl082172, 2019.
- 492 Shi, Z., Vu, T., Kothaus, S., Harrison, R. M., Grimmond, S., Yue, S., Zhu, T., Lee, J., Han, Y., Demuzere,
493 M., Dunmore, R. E., Ren, L., Liu, D., Wang, Y., Wild, O., Allan, J., Acton, W. J., Barlow, J., Barratt, B.,
494 Beddows, D., Blossey, W. J., Calzolai, G., Carruthers, D., Carslaw, D. C., Chan, Q., Chatzidiakou, L.,
495 Chen, Y., Crilley, L., Cee, H., Dai, T., Doherty, R., Duan, F., Fu, P., Ge, B., Ge, M., Guan, D., Hamilton,
496 J. F., He, K., Heal, M., Heard, D., Hewitt, C. N., Holloway, M., Hu, M., Ji, D., Jiang, X., Jones, R., Kalberer,
497 M., Kelly, F. J., Kramer, L., Langford, B., Lin, C., Lewis, A. C., Li, J., Li, W., Liu, H., Liu, J., Leh, M., Lu, K.,
498 Lucarelli, F., Mann, G., McFiggans, G., Miller, M. R., Mills, G., Monk, P., Nemitz, E., O'Connor, F.,
499 Ouyang, B., Palmer, P. I., Percival, C., Popelea, O., Reeves, C., Rickard, A. R., Shao, L., Shi, G.,
500 Spracklen, D., Stevenson, D., Sun, Y., Sun, Z., Tao, S., Tong, S., Wang, Q., Wang, W., Wang, X., Wang,
501 X., Wang, Z., Wei, L., Whalley, L., Wu, X., Wu, Z., Xie, P., Yang, F., Zhang, Q., Zhang, Y., Zhang, Y.,
502 and Zheng, M.: Introduction to the special issue “In-depth study of air pollution sources and
503 processes within Beijing and its surrounding region (APHH-Beijing)”, *Atmos. Chem. Phys.*, 19,
504 7519–7546, 10.5194/acp-19-7519-2019, 2019.
- 505 Sun, Y., Jiang, Q., Wang, Z., Fu, P., Li, J., Yang, T., and Yin, Y.: Investigation of the Sources and
506 Evolution Processes of Severe Haze Pollution in Beijing in January 2013, *Journal of Geophysical
507 Research: Atmospheres*, 2014JD021641, 10.1002/2014JD021641, 2014.
- 508 Sun, Y., Jiang, Q., Xu, Y., Ma, Y., Zhang, Y., Liu, X., Li, W., Wang, F., Li, J., Wang, P., and Li, Z.: Aerosol
509 characterization over the North China Plain: Haze life cycle and biomass burning impacts in
510 summer, *Journal of Geophysical Research: Atmospheres*, 121, 2508–2521, 10.1002/2015JD024261,
511 2016.
- 512 Sun, Y. L., Zhang, Q., Schwab, J. J., Chen, W. N., Bae, M. S., Hung, H. M., Lin, Y. C., Ng, N. L., Jayne,
513 J., Massoli, P., Williams, L. R., and Demerjian, K. L.: Characterization of near highway submicron
514 aerosols in New York City with a high-resolution aerosol mass spectrometer, *Atmos. Chem. Phys.*,
515 12, 2215–2227, 10.5194/acp-12-2215-2012, 2012.
- 516 Ullrich, I. M., Canagaratna, M. R., Zhang, Q., Worsnop, D. R., and Jimenez, J. L.: Interpretation of
517 organic components from Positive Matrix Factorization of aerosol mass spectrometric data, *Atmos.
518 Chem. Phys.*, 9, 2891–2918, 10.5194/acp-9-2891-2009, 2009.
- 519 V. Buxton, G., Bydder, M., and Arthur Salmon, G.: The reactivity of chlorine atoms in aqueous
520 solution Part II. The equilibrium $\text{SO}_4^{2-} + \text{Cl}^- \rightleftharpoons \text{ClN}(\text{SO}_4)_2$, *Physical Chemistry Chemical Physics*, 1,
521 269–273, 10.1039/A807808D, 1999.
- 522 Wang, J., Onasch, T. B., Ge, X., Collier, S., Zhang, Q., Sun, Y., Yu, H., Chen, M., Prévôt, A. S., and

- 523 Worsnop, D. R.: Observation of fullerene soot in eastern China, *Environmental Science &*
524 *Technology Letters*, 3, 121–126, 2016.
- 525 Wang, J., Zhang, Q., Chen, M., Collier, S., Zhou, S., Ge, X., Xu, J., Shi, J., Xie, C., and Hu, J.: First
526 chemical characterization of refractory black carbon aerosols and associated coatings over the
527 Tibetan Plateau (4720 m asl), *Environmental science & technology*, 51, 14072–14082, 2017.
- 528 Wang, J., Liu, D., Ge, X., Wu, Y., Shen, F., Chen, M., Zhao, J., Xie, C., Wang, Q., and Xu, W.:
529 Characterization of black carbon-containing fine particles in Beijing during wintertime,
530 *Atmospheric Chemistry and Physics*, 19, 447–458, 2019.
- 531 Willis, M. D., Lee, A. K. Y., Onasch, T. B., Fortner, E. C., Williams, L. R., Lambe, A. T., Worsnop, D. R.,
532 and Abbatt, J. P. D.: Collection efficiency of the soot particle aerosol mass spectrometer (SP-AMS)
533 for internally mixed particulate black carbon, *Atmos. Meas. Tech.*, 7, 4507–4516, 10.5194/amt-7-
534 4507–2014, 2014.
- 535 Wu, Y., Liu, D., Wang, J., Shen, F., Chen, Y., Cui, S., Ge, S., Wu, Y., Chen, M., and Ge, X.:
536 Characterization of Size Resolved Hygroscopicity of Black Carbon Containing Particle in Urban
537 Environment, *Environmental science & technology*, 53, 14212–14221, 2019.
- 538 Xie, C., Xu, W., Wang, J., Liu, D., Ge, X., Zhang, Q., Wang, Q., Du, W., Zhao, J., Zhou, W., Li, J., Fu, P.,
539 Wang, Z., Worsnop, D., and Sun, Y.: Light absorption enhancement of black carbon in urban Beijing
540 in summer, *Atmos Environ*, 213, 499–504, <https://doi.org/10.1016/j.atmosenv.2019.06.041>, 2019a.
- 541 Xie, C., Xu, W., Wang, J., Wang, Q., Liu, D., Tang, G., Chen, P., Du, W., Zhao, J., and Zhang, Y.:
542 Vertical characterization of aerosol optical properties and brown carbon in winter in urban Beijing,
543 China, *Atmospheric Chemistry and Physics*, 19, 165–179, 2019b.
- 544 Xu, J., Zhang, Q., Shi, J., Ge, X., Xie, C., Wang, J., Kang, S., Zhang, R., and Wang, Y.: Chemical
545 characteristics of submicron particles at the central Tibetan Plateau: insights from aerosol mass
546 spectrometry, *Atmospheric Chemistry and Physics*, 18, 2018.
- 547 Xu, W., Sun, Y., Wang, Q., Zhao, J., Wang, J., Ge, X., Xie, C., Zhou, W., Du, W., and Li, J.: Changes in
548 aerosol chemistry from 2014 to 2016 in winter in Beijing: Insights from high resolution aerosol
549 mass spectrometry, *Journal of Geophysical Research: Atmospheres*, 124, 1132–1147, 2019a.
- 550 Xu, W., Sun, Y., Wang, Q., Zhao, J., Wang, J., Ge, X., Xie, C., Zhou, W., Du, W., and Li, J.: Changes in
551 aerosol chemistry from 2014 to 2016 in winter in Beijing: Insights from high resolution aerosol
552 mass spectrometry, *J Geophys Res: Atmos*, 124, 1132–1147, 2019b.
- 553 Xu, W., Xie, C., Karnezi, E., Zhang, Q., Wang, J., Pandis, S. N., Ge, X., Zhang, J., An, J., and Wang, Q.:
554 Summertime aerosol volatility measurements in Beijing, China, *Atmos. Chem. Phys.*, 19, 10205–
555 10216, 2019c.
- 556 Xu, W., Xie, C., Karnezi, E., Zhang, Q., Wang, J., Pandis, S. N., Ge, X., Zhang, J., An, J., Wang, Q.,
557 Zhao, J., Du, W., Qiu, Y., Zhou, W., He, Y., Li, Y., Li, J., Fu, P., Wang, Z., Worsnop, D. R., and Sun, Y.:
558 Summertime aerosol volatility measurements in Beijing, China, *Atmos. Chem. Phys.*, 19, 10205–
559 10216, 10.5194/acp-19-10205-2019, 2019d.
- 560 Zhang, Q., Jimenez, J., Canagaratna, M., Ulbrich, I., Ng, N., Worsnop, D., and Sun, Y.: Understanding
561 atmospheric organic aerosols via factor analysis of aerosol mass spectrometry: a review, *Analytical
562 and Bioanalytical Chemistry*, 401, 3045–3067, 10.1007/s00216-011-5355-y, 2011.

References

- 563 Bond, T. C., Doherty, S. J., Fahey, D. W., Forster, P. M., Berntsen, T., DeAngelo, B. J., Flanner, M.
564 Ghan, S., Kärcher, B., Koch, D., Kinne, S., Kondo, Y., Quinn, P. K., Sarofim, M. C., Schultz, M.
565 G., Schulz, M., Venkataraman, C., Zhang, H., Zhang, S., Bellouin, N., Guttikunda, S. K., Hopke, P.

566 [K., Jacobson, M. Z., Kaiser, J. W., Klimont, Z., Lohmann, U., Schwarz, J. P., Shindell, D., Storelvmo, T., Warren, S. G., and Zender, C. S.: Bounding the role of black carbon in the climate system: A scientific assessment, J. Geophys. Res.- Atmos., 118, 5380-5552, 10.1002/jgrd.50171, 2013.](#)

567 [Busbeck, P. R., Adachi, K., Gelencsér, A., Tompa, É., and Pósfai, M.: Ns-Soot: A Material-Based](#)

568 [Term for Strongly Light-Absorbing Carbonaceous Particles, Aerosol Sci. Technol., 48, 777-788, 10.1080/02786826.2014.919374, 2014.](#)

569 [Canagaratna, M. R., Jayne, J. T., Jimenez, J. L., Allan, J. D., Alfarra, M. R., Zhang, Q., Onasch, T. B., Drewnick, F., Coe, H., Middlebrook, A., Delia, A., Williams, L. R., Trimborn, A. M., Northway, M. J., DeCarlo, P. F., Kolb, C. E., Davidovits, P., and Worsnop, D. R.: Chemical and microphysical](#)

570 [characterization of ambient aerosols with the aerodyne aerosol mass spectrometer, Mass Spectrom. Rev., 26, 185-222, 10.1002/Mas.20115, 2007.](#)

571 [Canagaratna, M. R., Jimenez, J. L., Kroll, J. H., Chen, Q., Kessler, S. H., Massoli, P., Hildebrandt Ruiz, L., Fortner, E., Williams, L. R., Wilson, K. R., Surratt, J. D., Donahue, N. M., Jayne, J. T., and Worsnop, D. R.: Elemental ratio measurements of organic compounds using aerosol mass spectrometry: characterization, improved calibration, and implications, Atmos. Chem. Phys., 15, 253-272, 10.5194/acp-15-253-2015, 2015a.](#)

572 [Canagaratna, M. R., Massoli, P., Browne, E. C., Franklin, J. P., Wilson, K. R., Onasch, T. B., Kirchstetter, T. W., Fortner, E. C., Kolb, C. E., Jayne, J. T., Kroll, J. H., and Worsnop, D. R.: Chemical Compositions of Black Carbon Particle Cores and Coatings via Soot Particle Aerosol](#)

573 [Mass Spectrometry with Photoionization and Electron Ionization, J. Phys. Chem. A, 119, 4589-4599, 10.1021/jp510711u, 2015b.](#)

574 [Cappa, C. D., Onasch, T. B., Massoli, P., Worsnop, D. R., Bates, T. S., Cross, E. S., Davidovits, P., Hakala, J., Hayden, K. L., Jobson, B. T., Kolesar, K. R., Lack, D. A., Lerner, B. M., Li, S.-M., Mellon, D., Nuaaman, I., Olfert, J. S., Petäjä, T., Quinn, P. K., Song, C., Subramanian, R., Williams, E. J., and Zaveri, R. A.: Radiative absorption enhancements due to the mixing state of atmospheric](#)

575 [black carbon, Science, 337, 1078-1081, 10.1126/science.1223447, 2012.](#)

576 [Chen, B., Andersson, A., Lee, M., Kirillova, E. N., Xiao, Q., Kruså, M., Shi, M., Hu, K., Lu, Z., Streets, D. G., Du, K., and Gustafsson, Ö.: Source Forensics of Black Carbon Aerosols from China, Environ. Sci. Technol., 47, 9102-9108, 10.1021/es401599r, 2013.](#)

577 [Chen, Y.; Cai, J.; Wang, Z.; Peng, C.; Yao, X.; Tian, M.; Han, Y.; Shi, G.; Shi, Z.; Liu, Y.; Yang, X.; Zheng, M.; Zhu, T.; He, K.; Zhang, Q.; Yang, F. Simultaneous measurements of urban and rural](#)

578 [particles in Beijing – Part 1: Chemical composition and mixing state, Atmos. Chem. Phys., 20, 9231-9247, 10.5194/acp-20-9231-2020, 2020a.](#)

579 [Chen, Y.; Shi, G.; Cai, J.; Shi, Z.; Wang, Z.; Yao, X.; Tian, M.; Peng, C.; Han, Y.; Zhu, T.; Liu, Y.; Yang, X.; Zheng, M.; Yang, F.; Zhang, Q.; He, K. Simultaneous measurements of urban and rural](#)

580 [particles in Beijing – Part 2: Case studies of haze events and regional transport, Atmos. Chem. Phys., 20, 9249-9263, 10.5194/acp-20-9249-2020, 2020b.](#)

581 [China, S., Scarnato, B., Owen, R. C., Zhang, B., Ampadu, M. T., Kumar, S., Dzepina, K., Dziobak, M. P., Fialho, P., Perlinger, J. A., Hueber, J., Helmig, D., Mazzoleni, L. R., and Mazzoleni, C.: Morphology and mixing state of aged soot particles at a remote marine free troposphere site: Implications for optical properties, Geophys. Res. Lett., 42, 1243-1250, 10.1002/2014gl062404, 2015.](#)

582 [Collier, S., Zhou, S., Kuwayama, T., Forestieri, S., Brady, J., Zhang, M., Kleeman, M., Cappa, C., Bertram, T., and Zhang, Q.: Organic PM Emissions from Vehicles: Composition, O/C Ratio, and](#)

610 [Dependence on PM Concentration, Aerosol Sci. Technol., 49, 86-97, 10.1080/02786826.2014.1003364, 2015.](#)

611 [Ge, X., Zhang, Q., Sun, Y., Ruehl, C. R., and Setyan, A.: Effect of aqueous-phase processing on aerosol chemistry and size distributions in Fresno, California, during wintertime, Environ. Chem., 9, 221-235, <http://dx.doi.org/10.1071/EN11168>, 2012a.](#)

612 [Ge, X. L., Setyan, A., Sun, Y., and Zhang, Q.: Primary and secondary organic aerosols in Fresno, California during wintertime: Results from high resolution aerosol mass spectrometry, J. Geophys. Res.-Atmos., 117, D19301, \[10.1029/2012jd018026\]\(https://doi.org/10.1029/2012jd018026\), 2012b.](#)

613 [Janssen, N.A.H., Gerlofs-Nijland, M., Lanki, T., Salonen, R.O., Cassee, F., Hoek, G., Fischer, P., Brunekreef, B., Krzyzanowski, M., Health effects of black carbon, WHO, 2012. \[https://www.euro.who.int/_data/assets/pdf_file/0004/162535/e96541.pdf?ua=1\]\(https://www.euro.who.int/_data/assets/pdf_file/0004/162535/e96541.pdf?ua=1\)](#)

614 [Lee, A. K. Y., Chen, C. L., Liu, J., Price, D. J., Betha, R., Russell, L. M., Zhang, X., and Cappa, C. D.: Formation of secondary organic aerosol coating on black carbon particles near vehicular emissions, Atmos. Chem. Phys., 17, 15055-15067, \[10.5194/acp-17-15055-2017\]\(https://doi.org/10.5194/acp-17-15055-2017\), 2017.](#)

615 [Lee, B. P., Li, Y. J., Yu, J. Z., Louie, P. K. K., and Chan, C. K.: Physical and chemical characterization of ambient aerosol by HR-ToF-AMS at a suburban site in Hong Kong during springtime 2011, Journal of Geophysical Research: Atmospheres, n/a-n/a, \[10.1002/jgrd.50658\]\(https://doi.org/10.1002/jgrd.50658\), 2013.](#)

616 [Li, W. J., Shao, L. Y., and Buseck, P. R.: Haze types in Beijing and the influence of agricultural biomass burning, Atmos. Chem. Phys., 10, 8119-8130, \[10.5194/acp-10-8119-2010\]\(https://doi.org/10.5194/acp-10-8119-2010\), 2010.](#)

617 [Li, Y. J., Lee, B. P., Su, L., Fung, J. C. H., and Chan, C. K.: Seasonal characteristics of fine particulate matter \(PM\) based on high-resolution time-of-flight aerosol mass spectrometric \(HR-ToF-AMS\) measurements at the HKUST Supersite in Hong Kong, Atmos. Chem. Phys., 15, 37-53, \[10.5194/acp-15-37-2015\]\(https://doi.org/10.5194/acp-15-37-2015\), 2015.](#)

618 [Liu, C., Chung, C. E., Yin, Y., and Schnaiter, M.: The absorption Ångström exponent of black carbon: from numerical aspects, Atmos. Chem. Phys., 18, 6259-6273, \[10.5194/acp-18-6259-2018\]\(https://doi.org/10.5194/acp-18-6259-2018\), 2018.](#)

619 [Liu, D., Whitehead, J., Alfarra, M. R., Revesz-Villegas, E., Spracklen, Dominick V., Reddington, Carly L., Kong, S., Williams, Paul I., Ting, Y.-C., Haslett, S., Taylor, Jonathan W., Flynn, Michael J., Morgan, William T., McFiggans, G., Coe, H., and Allan, James D.: Black-carbon absorption enhancement in the atmosphere determined by particle mixing state, Nature Geosci., 10, 184-188, \[10.1038/ngeo2901\]\(https://doi.org/10.1038/ngeo2901\), 2017.](#)

620 [Liu, D., Joshi, R., Wang, J., Yu, C., Allan, J. D., Coe, H., Flynn, M. J., Xie, C., Lee, J., and Squires, F.: Contrasting physical properties of black carbon in urban Beijing between winter and summer, Atmos. Chem. Phys., 19, 6749-6769, 2019.](#)

621 [Massoli, P., Onasch, T. B., Cappa, C. D., Nuamaan, I., Hakala, J., Hayden, K., Li, S.-M., Sueper, D. T., Bates, T. S., Quinn, P. K., Jayne, J. T., and Worsnop, D. R.: Characterization of black carbon-containing particles from soot particle aerosol mass spectrometer measurements on the R/V Atlantis during CalNex 2010, J. Geophys. Res.-Atmos., 120, \[2014JD022834\]\(https://doi.org/10.1029/2014JD022834\), 2015.](#)

622 [Ng, N. L., Canagaratna, M. R., Jimenez, J. L., Chhabra, P. S., Seinfeld, J. H., and Worsnop, D. R.: Changes in organic aerosol composition with aging inferred from aerosol mass spectra, Atmos. Chem. Phys., 11, 6465-6474, \[10.5194/acp-11-6465-2011\]\(https://doi.org/10.5194/acp-11-6465-2011\), 2011.](#)

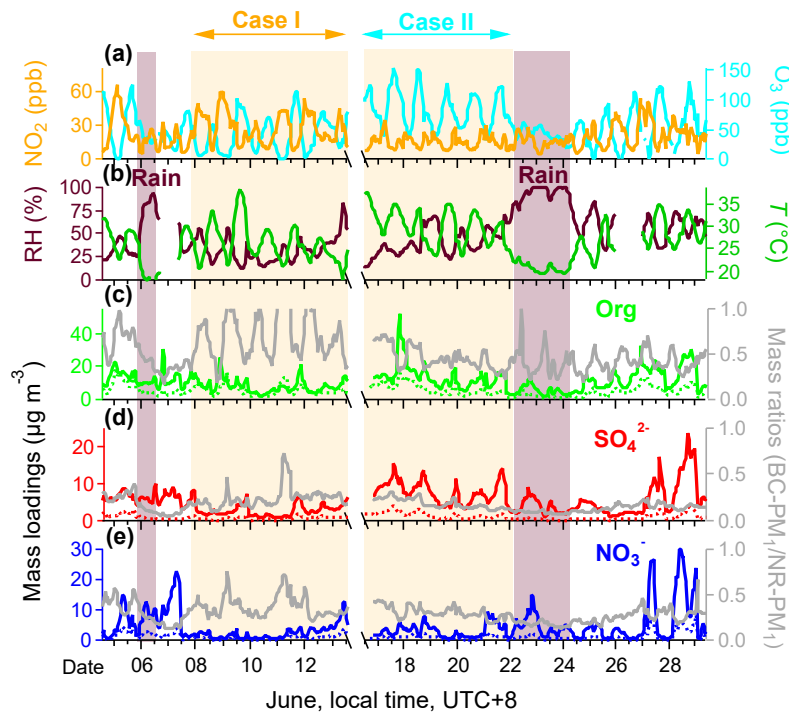
623 [Onasch, T. B., Trimborn, A., Fortner, E. C., Jayne, J. T., Kok, G. L., Williams, L. R., Davidovits, P., and Worsnop, D. R.: Soot Particle Aerosol Mass Spectrometer: Development, Validation, and Initial Application, Aerosol Science and Technology, 46, 804-817, \[10.1080/02786826.2012.663948\]\(https://doi.org/10.1080/02786826.2012.663948\), 2012.](#)

624 [Paatero, P., and Tapper, U.: Positive matrix factorization: A non-negative factor model with optimal](#)

- 654 [utilization of error estimates of data values, Environmetrics, 5, 111-126, 10.1002/env.3170050203, 1994.](#)
- 655 [Qiu, Y., Xie, Q., Wang, J., Xu, W., Li, L., Wang, Q., Zhao, J., Chen, Y., Chen, Y., Wu, Y., Du, W., Zhou, W., Lee, J., Zhao, C., Ge, X., Fu, P., Wang, Z., Worsnop, D. R., and Sun, Y.: Vertical Characterization and Source Apportionment of Water-Soluble Organic Aerosol with High-resolution Aerosol Mass Spectrometry in Beijing, China, ACS Earth Space Chem., 3, 273-284, 10.1021/acsearthspacechem.8b00155, 2019.](#)
- 656 [Ramanathan, V., and Carmichael, G.: Global and regional climate changes due to black carbon, Nature Geosci., 1, 221-227, 2008.](#)
- 657 [Saleh, R., Marks, M., Heo, J., Adams, P. J., Donahue, N. M., and Robinson, A. L.: Contribution of brown carbon and lensing to the direct radiative effect of carbonaceous aerosols from biomass and biofuel burning emissions, J. Geophys. Res.- Atmos., 120, 10.285-210.296, 10.1002/2015jd023697, 2015.](#)
- 658 [Shen, L., Jacob, D. J., Zhu, L., Zhang, Q., Zheng, B., Sulprizio, M. P., Li, K., De Smedt, I., González Abad, G., Cao, H., Fu, T.-M., and Liao, H.: The 2005–2016 Trends of Formaldehyde Columns Over China Observed by Satellites: Increasing Anthropogenic Emissions of Volatile Organic Compounds and Decreasing Agricultural Fire Emissions, Geophys. Res. Lett., 46, 4468-4475, 10.1029/2019gl082172, 2019.](#)
- 659 [Shi, Z., Vu, T., Kotthaus, S., Harrison, R. M., Grimmond, S., Yue, S., Zhu, T., Lee, J., Han, Y., Demuzere, M., Dunmore, R. E., Ren, L., Liu, D., Wang, Y., Wild, O., Allan, J., Acton, W. J., Barlow, J., Barratt, B., Beddows, D., Bloss, W. J., Calzolai, G., Carruthers, D., Carslaw, D. C., Chan, Q., Chatzidiakou, L., Chen, Y., Crilley, L., Coe, H., Dai, T., Doherty, R., Duan, F., Fu, P., Ge, B., Ge, M., Guan, D., Hamilton, J. F., He, K., Heal, M., Heard, D., Hewitt, C. N., Hollaway, M., Hu, M., Ji, D., Jiang, X., Jones, R., Kalberer, M., Kelly, F. J., Kramer, L., Langford, B., Lin, C., Lewis, A. C., Li, J., Li, W., Liu, H., Liu, J., Loh, M., Lu, K., Lucarelli, F., Mann, G., McFiggans, G., Miller, M., Mills, G., Monk, P., Nemitz, E., O'Connor, F., Ouyang, B., Palmer, P. I., Percival, C., Popoola, O., Reeves, C., Rickard, A. R., Shao, L., Shi, G., Spracklen, D., Stevenson, D., Sun, Y., Sun, Z., Tao, S., Tong, S., Wang, Q., Wang, W., Wang, X., Wang, X., Wang, Z., Wei, L., Whalley, L., Wu, X., Wu, Z., Xie, P., Yang, F., Zhang, Q., Zhang, Y., Zhang, Y., and Zheng, M.: Introduction to the special issue “In-depth study of air pollution sources and processes within Beijing and its surrounding region \(APHH-Beijing\)”, Atmos. Chem. Phys., 19, 7519-7546, 10.5194/acp-19-7519-2019, 2019.](#)
- 660 [Sun, Y., Jiang, Q., Wang, Z., Fu, P., Li, J., Yang, T., and Yin, Y.: Investigation of the Sources and Evolution Processes of Severe Haze Pollution in Beijing in January 2013, J. Geophys. Res.- Atmos., 2014JD021641, 10.1002/2014JD021641, 2014.](#)
- 661 [Sun, Y., Jiang, Q., Xu, Y., Ma, Y., Zhang, Y., Liu, X., Li, W., Wang, F., Li, J., Wang, P., and Li, Z.: Aerosol characterization over the North China Plain: Haze life cycle and biomass burning impacts in summer, J. Geophys. Res.- Atmos., 121, 2508-2521, 10.1002/2015jd024261, 2016.](#)
- 662 [Sun, Y. L., Zhang, Q., Schwab, J. J., Chen, W. N., Bae, M. S., Hung, H. M., Lin, Y. C., Ng, N. L., Jayne, J., Massoli, P., Williams, L. R., and Demerjian, K. L.: Characterization of near-highway submicron aerosols in New York City with a high-resolution aerosol mass spectrometer, Atmos. Chem. Phys., 12, 2215-2227, 10.5194/acp-12-2215-2012, 2012.](#)
- 663 [Ulbrich, I. M., Canagaratna, M. R., Zhang, Q., Worsnop, D. R., and Jimenez, J. L.: Interpretation of organic components from Positive Matrix Factorization of aerosol mass spectrometric data, Atmos. Chem. Phys., 9, 2891-2918, 10.5194/acp-9-2891-2009, 2009.](#)
- 664
- 665
- 666
- 667
- 668
- 669
- 670
- 671
- 672
- 673
- 674
- 675
- 676
- 677
- 678
- 679
- 680
- 681
- 682
- 683
- 684
- 685
- 686
- 687
- 688
- 689
- 690
- 691
- 692
- 693
- 694
- 695
- 696
- 697

- 698 [V. Buxton, G., Bydder, M., and Arthur Salmon, G.: The reactivity of chlorine atoms in aqueous](#)
699 [solution. Part II. The equilibrium \$\text{SO}_4^{\cdot-} + \text{Cl}^{\cdot} \text{Cl}^{\text{Nsbd}} + \text{SO}_4^{2-}\$, Phys. Chem. Chem. Phys., 1, 269-273,](#)
700 [10.1039/A807808D, 1999.](#)
- 701 [Wang, J., Onasch, T. B., Ge, X., Collier, S., Zhang, Q., Sun, Y., Yu, H., Chen, M., Prévôt, A. S., and](#)
702 [Worsnop, D. R.: Observation of fullerene soot in eastern China, Environ. Sci. Technol. Lett., 3, 121-](#)
703 [126, 10.1021/acs.estlett.6b00044, 2016.](#)
- 704 [Wang, J., Zhang, Q., Chen, M., Collier, S., Zhou, S., Ge, X., Xu, J., Shi, J., Xie, C., and Hu, J.: First](#)
705 [chemical characterization of refractory black carbon aerosols and associated coatings over the](#)
706 [Tibetan Plateau \(4730 m asl\), Environ. Sci. Technol., 51, 14072-14082, 10.1021/acs.est.7b03973,](#)
707 [2017.](#)
- 708 [Wang, J., Liu, D., Ge, X., Wu, Y., Shen, F., Chen, M., Zhao, J., Xie, C., Wang, Q., and Xu, W.:](#)
709 [Characterization of black carbon-containing fine particles in Beijing during wintertime, Atmos.](#)
710 [Chem. Phys., 19, 447-458, 10.5194/acp-19-447-2019, 2019.](#)
- 711 [Willis, M. D., Lee, A. K. Y., Onasch, T. B., Fortner, E. C., Williams, L. R., Lambe, A. T., Worsnop,](#)
712 [D. R., and Abbatt, J. P. D.: Collection efficiency of the soot-particle aerosol mass spectrometer \(SP-](#)
713 [AMS\) for internally mixed particulate black carbon, Atmos. Meas. Tech., 7, 4507-4516,](#)
714 [10.5194/amt-7-4507-2014, 2014.](#)
- 715 [Wu, Y., Liu, D., Wang, J., Shen, F., Chen, Y., Cui, S., Ge, S., Wu, Y., Chen, M., and Ge, X.:](#)
716 [Characterization of Size-Resolved Hygroscopicity of Black Carbon-Containing Particle in Urban](#)
717 [Environment, Environ. Sci. Technol., 53, 14212-14221, 10.1021/acs.est.9b05546, 2019.](#)
- 718 [Xie, C., Xu, W., Wang, J., Liu, D., Ge, X., Zhang, Q., Wang, Q., Du, W., Zhao, J., Zhou, W., Li, J.,](#)
719 [Fu, P., Wang, Z., Worsnop, D., and Sun, Y.: Light absorption enhancement of black carbon in urban](#)
720 [Beijing in summer, Atmos. Environ., 213, 499-504, 10.1016/j.atmosenv.2019.06.041, 2019a.](#)
- 721 [Xie, C., Xu, W., Wang, J., Wang, Q., Liu, D., Tang, G., Chen, P., Du, W., Zhao, J., and Zhang, Y.:](#)
722 [Vertical characterization of aerosol optical properties and brown carbon in winter in urban Beijing,](#)
723 [China, Atmos. Chem. Phys., 19, 165-179, 10.5194/acp-19-165-2019, 2019b.](#)
- 724 [Xu, J., Zhang, Q., Shi, J., Ge, X., Xie, C., Wang, J., Kang, S., Zhang, R., and Wang, Y.: Chemical](#)
725 [characteristics of submicron particles at the central Tibetan Plateau: insights from aerosol mass](#)
726 [spectrometry, Atmos. Chem. Phys., 18, 427-443, 10.5194/acp-18-427-2018, 2018.](#)
- 727 [Xu, W., Sun, Y., Wang, Q., Zhao, J., Wang, J., Ge, X., Xie, C., Zhou, W., Du, W., and Li, J.: Changes](#)
728 [in aerosol chemistry from 2014 to 2016 in winter in Beijing: Insights from high-resolution aerosol](#)
729 [mass spectrometry, J. Geophys. Res.-Atmos., 124, 1132-1147, 10.1029/2018JD029245, 2019a.](#)
- 730 [Xu, W., Xie, C., Karnezi, E., Zhang, Q., Wang, J., Pandis, S. N., Ge, X., Zhang, J., An, J., and Wang,](#)
731 [Q.: Summertime aerosol volatility measurements in Beijing, China, Atmos. Chem. Phys., 19, 10205-](#)
732 [10216, 10.5194/acp-19-10205-2019, 2019b.](#)
- 733 [Zhang, Q., Jimenez, J., Canagaratna, M., Ulbrich, I., Ng, N., Worsnop, D., and Sun, Y.:](#)
734 [Understanding atmospheric organic aerosols via factor analysis of aerosol mass spectrometry: a](#)
735 [review, Anal. Bioanal. Chem., 401, 3045-3067, 10.1007/s00216-011-5355-y, 2011.](#)

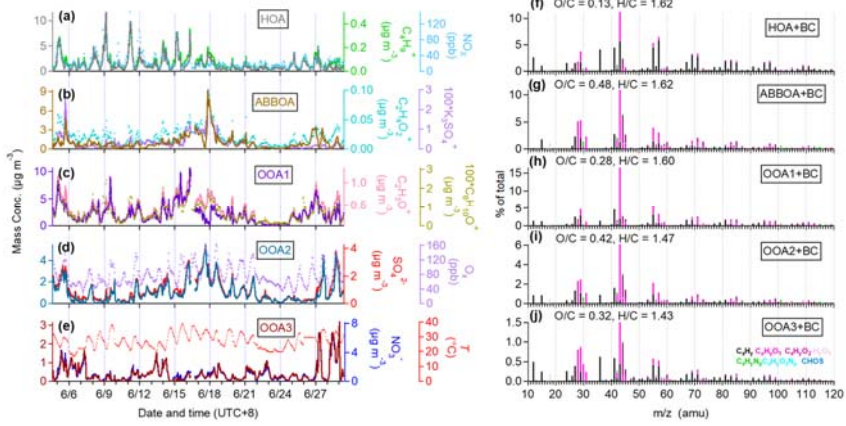
736



737

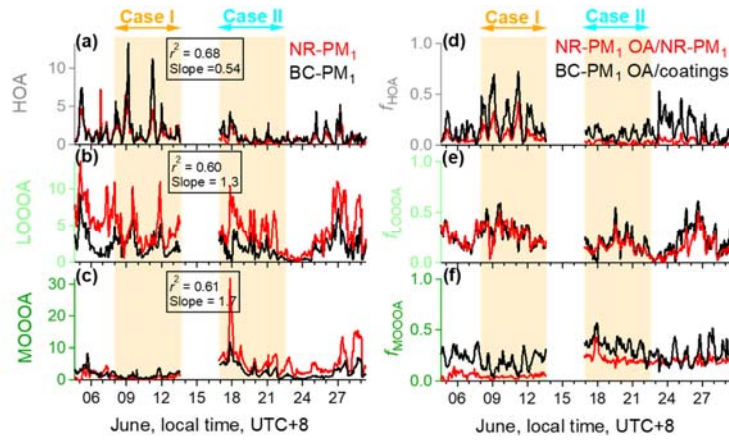
738 **Figure 1.** Temporal variations of selected chemical species measured in Beijing on June 4 -29, 2017.

739 (a) mixing ratios of nitrogen dioxide (NO_2) and ozone (O_3); (b) 15-m relative humidity (RH) and
 740 temperature (T); (c-e) on the left are the mass loadings of organic (Org), sulfate (SO_4^{2-}) and nitrate
 741 (NO_3^-) measured by HR-AMS and SP-AMS, and on the right are mass ratios of individual BC-PM_1
 742 species to NR-PM_1 species (e.g., BC-PM_1 Org to NR-PM_1 Org). The NR-PM_1 species measured by
 743 HR-AMS is in solid line, and the BC-PM_1 species measured by SP-AMS is in the dotted line. The
 744 shaded areas are raining periods. The observation period is divided into two cases according to the
 745 mixing ratio of nitrogen NO_2 , Case I and Case II, which represent high NO_2 and low NO_2 mixing
 746 ratios, respectively.



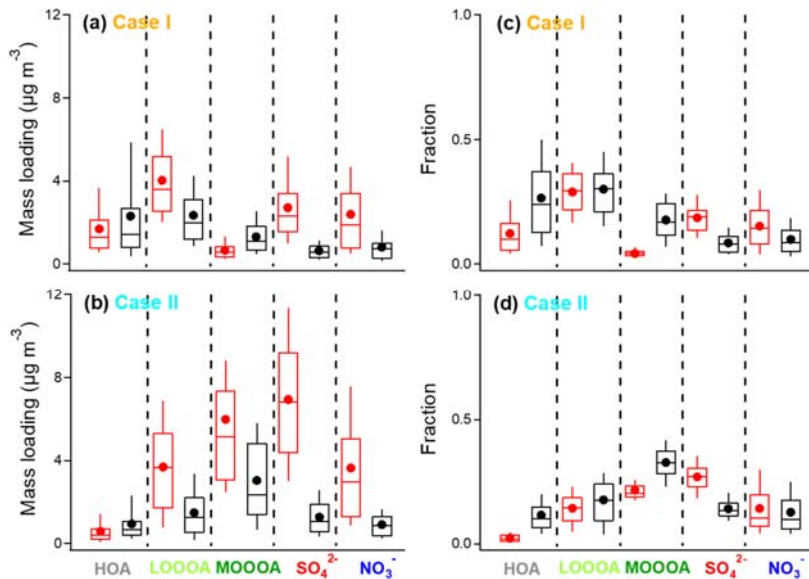
747

748 **Figure 2.** Temporal variations (left panels), high-resolution mass spectra (right panels) of five OA
 749 factors in summer 2017: (a) and (f) HOA, (b) and (g) A-BBOA, (c) and (h) OOA1 (LO-OOA), (d)
 750 and (i) OOA2, and (e) and (j) OOA3. Also shown in the left panels are the time series of other
 751 tracers, including C₄H₉⁺, NOx, C₂H₄O₂⁺, K₃SO₄⁺, C₆H₁₀O⁺, C₂H₃O⁺, SO₄²⁻ and NO₃⁻.



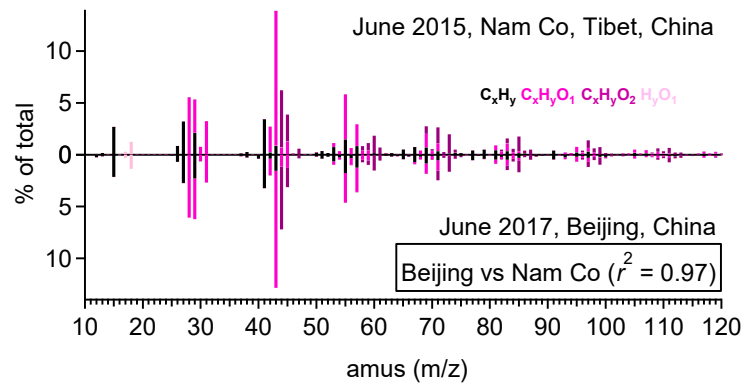
752

753 **Figure 3.** Temporal variations of NR-PM₁ and BC-PM₁ (a-c) HOA, LO-OOA, and MO-OOA (left
 754 panels) and (d-e) their fractions. NR-PM₁ OA factors are in red, and the BC-PM₁ OA factors are in
 755 black. Here BC-PM₁ MO-OOA is the sum of A-BBOA, OOA2 (sulfate-related OOA), and OOA3
 756 (nitrate-related OOA).



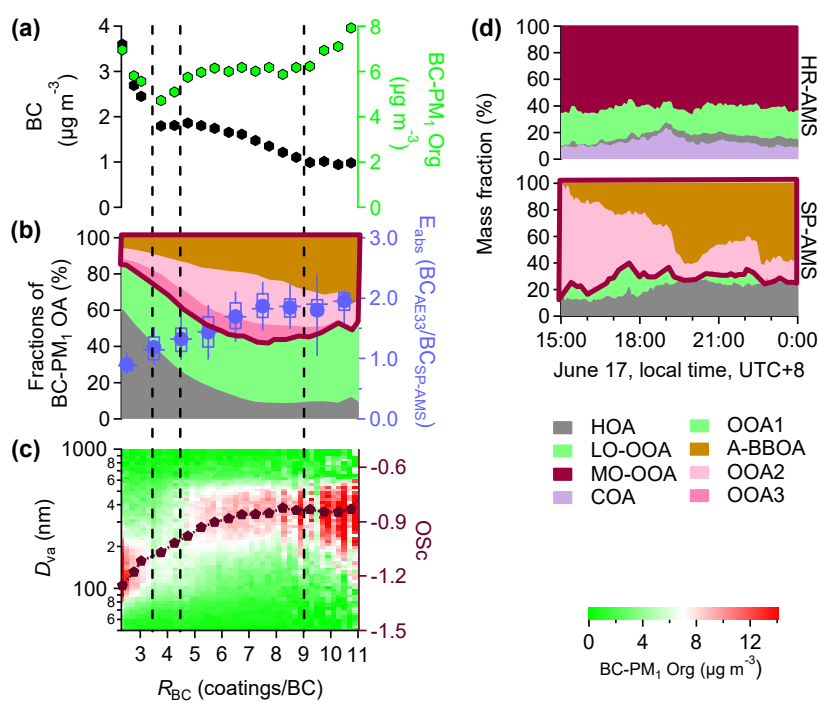
757

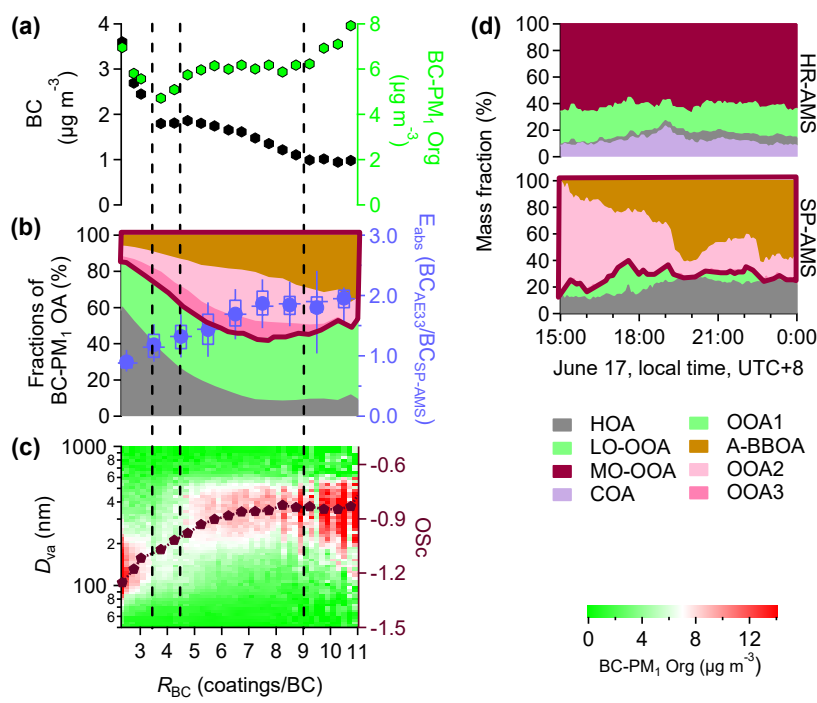
758 **Figure 4.** Box plots of mass loadings and fractions of five selected species (HOA, LO-OOA, MO-
 759 OOA, SO_4^{2-} , and NO_3^-) in Case I and Case II. The bounds of boxes represent quartiles, the whiskers
 760 indicate the 90th and 10th percentiles, and the lines and dots inside the boxes are median and mean
 761 values. NR-PM₁ OA factors are in red, and the BC-PM₁ OA factors are in black.



762

763 **Figure 5** Comparison between the high-resolution mass spectra of A-BBOA obtained in Nam Co
764 (June 2015) and Beijing (June 2017) (nitrogen-containing ions are not shown here).





766
767 **Figure 6.** (a-c) the mass loadings of BC, BC-PM₁ Org, fractions of BC-PM₁ OA factors, E_{abs} , the
768 oxidation state ($\text{OSc} = 2*(\text{O/C}) - (\text{H/C})$) of BC-PM₁ Org, and the size distribution of BC-PM₁ Org
769 as a function of coating thickness (R_{BC}). (d) temporal variations of OA fractions of NR-PM₁ and
770 BC-PM₁ from 15:00 to 24:00 on June 17, 2017.

771
772 带格式的: 字体: +西文正文(等线), 五号, 字体颜色: 自动
 带格式的: 行距: 单倍行距, 不取消行号